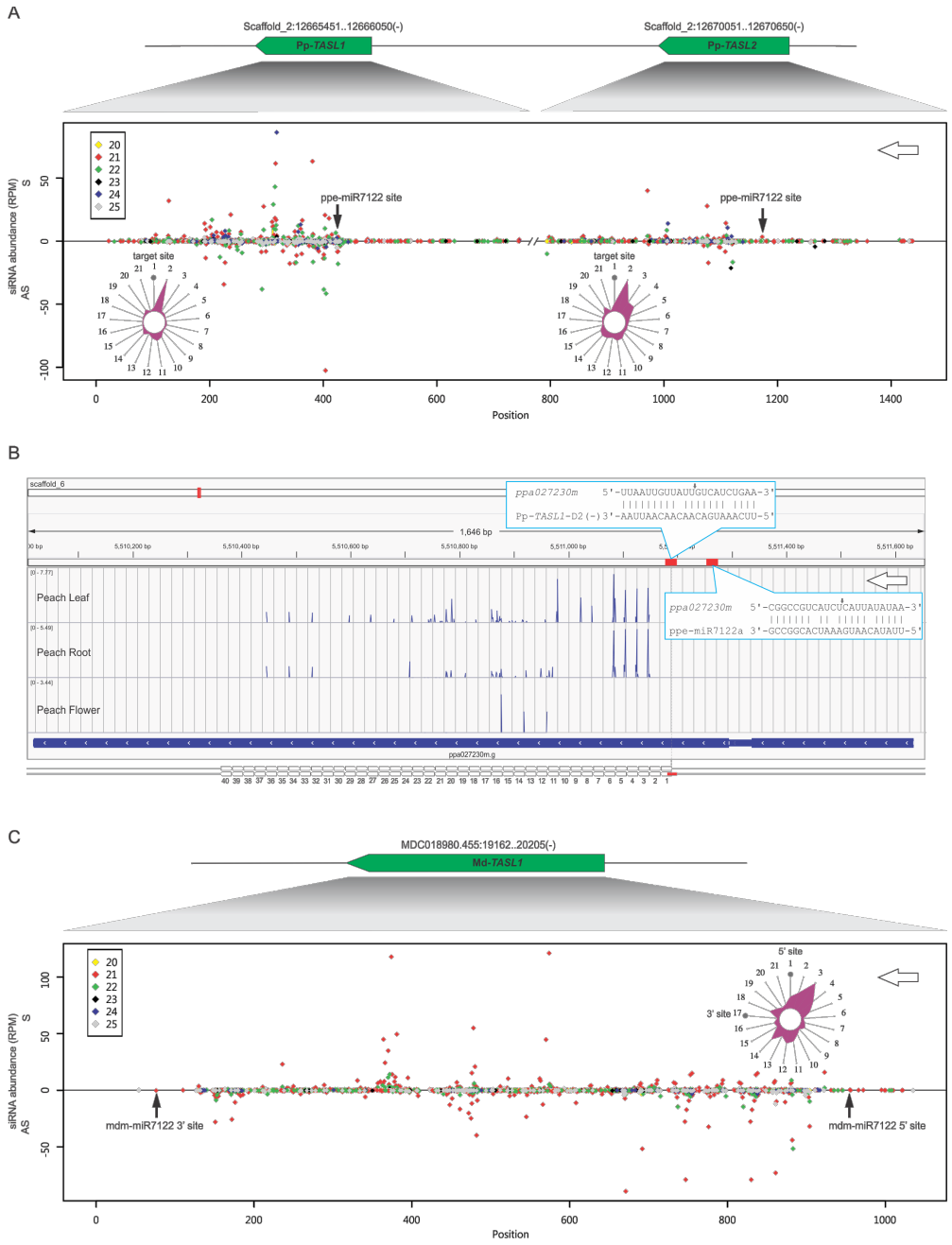

Supplemental Figure 1. siRNA distribution along Pp-*TASL1/2*, a peach *PPR* gene and Md-*TASL1*

(A/C) Dot plots and radar charts illustrating the siRNA production of Pp-*TASL1/2* (A) and Md-*TASL1* (C). Target sites of miR7122 are indicated by small black arrows. Radar chart displays the abundance of reads corresponding to each of the 21 possible phasing registers, with the 5' end of the miRNA trigger guided cleavage of the target site defined as register 1. The total number of small RNAs mapping to that register is plotted as relative distance from the center. The transcript direction is denoted by large arrows at the upper-right corner.

(B) Phasing score distribution along a peach *PHAS PPR* gene (ppa027230m). Parings of miRNA or tasiRNA and their target sites are denoted; grey gridlines show the 21-nt phasing pattern set up by the cleavage site of the Pp-*TASL1*-D2(-). A diagram showing the siRNA production pattern after the potential cleavage guided by the Pp-*TASL1*-D2(-) is included below.

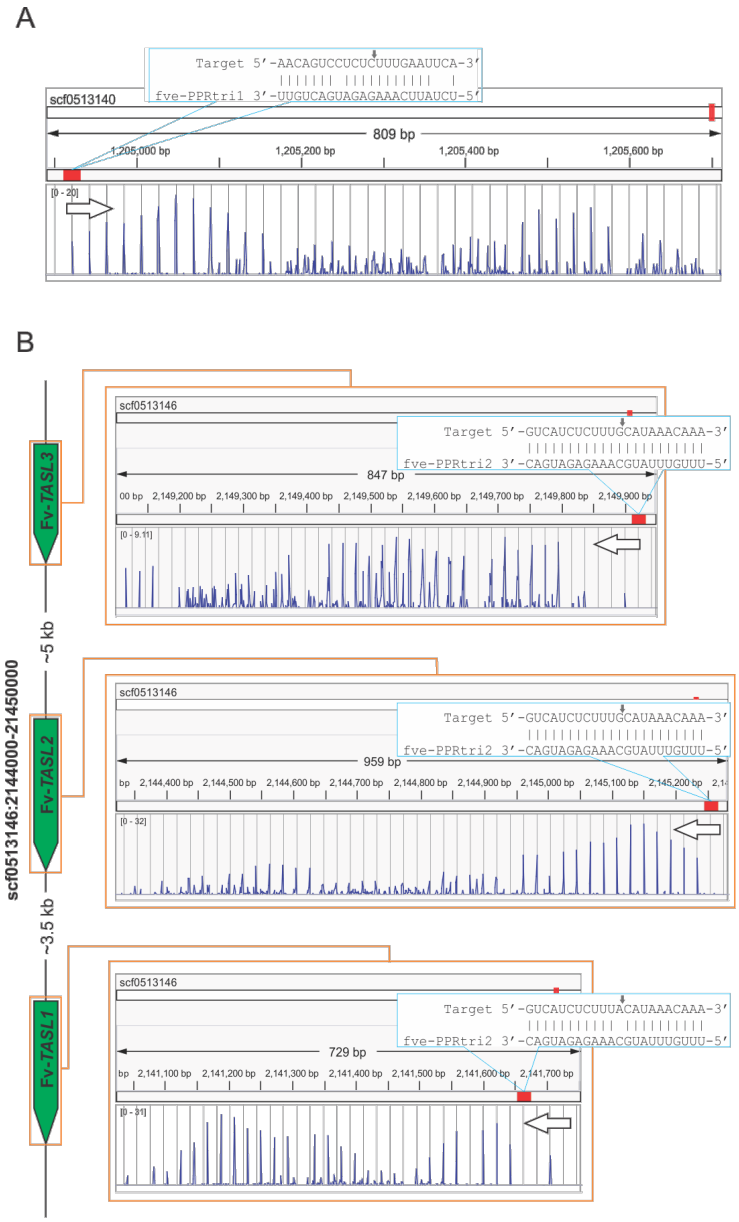

Supplemental Figure 2. The miRNA-*TASL-PPR*-siRNA pathway is conserved in strawberry

Phasing score distribution along a *PHAS PPR* gene (A) and three *TAS*-like loci (B) in strawberry. Pairings of fve-PPRtri1 or 2 and target sites are indicated correspondingly; genomic configuration of three *TAS*-like loci is denoted on the right of panel B; grey gridlines show the 21-nt phasing pattern set up by the cleavage site of fve-PPRtri1 or 2. The transcript direction is denoted by large arrows on the left or right side.

Supplemental Figure 3. Two layers of trans-acting interaction involved in the miR1509-*TASL-PPR*-siRNA pathway in soybean and Medicago.

Phasing score distribution along *TASL-L1*s, *TASL-L2*s and *PPR*s are viewed together with PARE data in IGV. Parings of the trigger (miRNA or tasiRNA) and the target site are denoted for each gene with cleavage site marked with a small red arrow; grey gridline show the 21-nt phasing pattern set up by the cleavage site of the corresponding trigger. Uncleaved target site of *TASL-L1*s are indicated in grey boxes. Diagrams showing the siRNA production pattern after the cleavage guided by trigger miRNAs or tasiRNAs are included below; tasiRNAs serving as triggers of next-layer *TASL* or *PPR* genes are highlighted in yellow. Red bars in the PARE data track indicates the values corresponding to the cleavage site of trigger miRNAs or tasiRNAs. The transcript direction is denoted by large arrows on the left or right side.

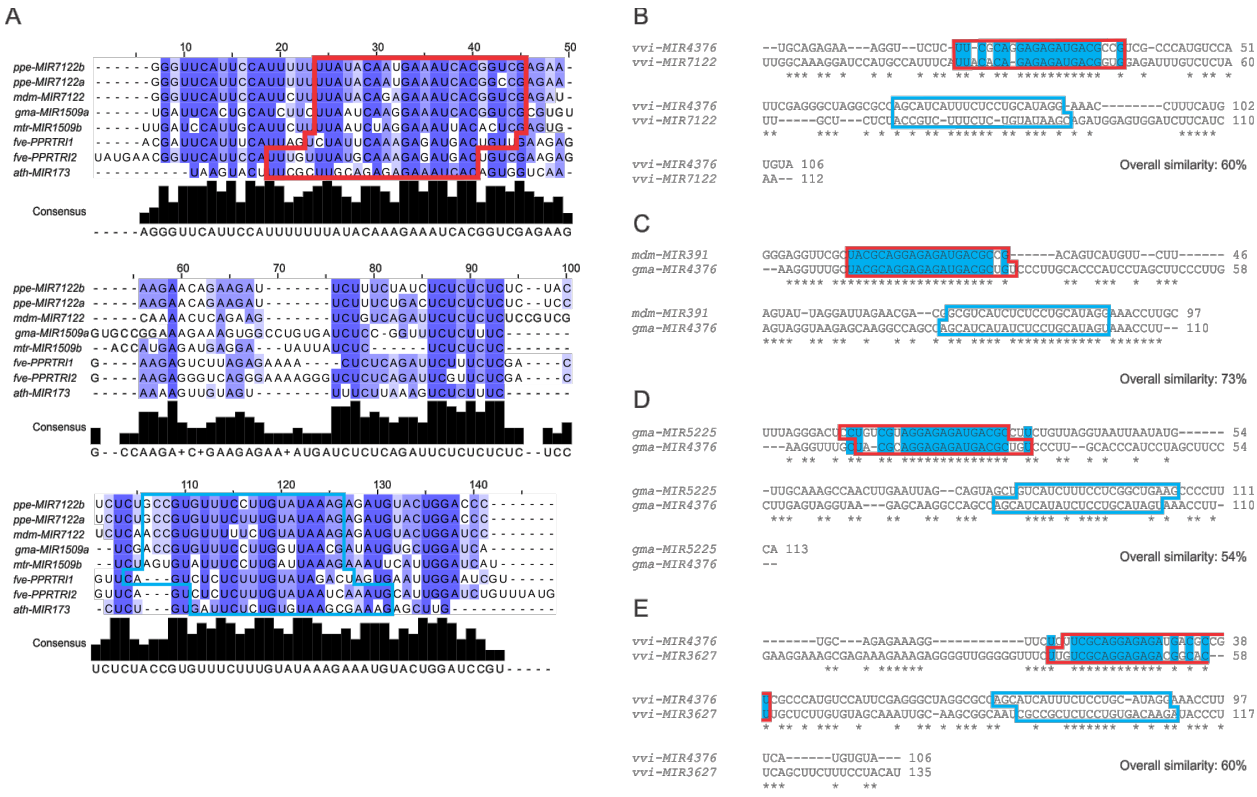

Supplemental Figure 4. Alignment of *MIRNA* genes.

(A) Full view of multiple alignment of foldback sequences of eight *MIRNA* genes, with miRNA and miRNA* marked in red and light-blue boxes, respectively.

(B-E) Pairwise alignment of foldback sequences of *MIRNA* genes. Sequences of miRNA and miRNA* are highlighted in red or light-blue boxes, respectively; identical nucleotides within the miRNA aligned region are marked in light blue. Overall similarity for each pair is included below each panel.

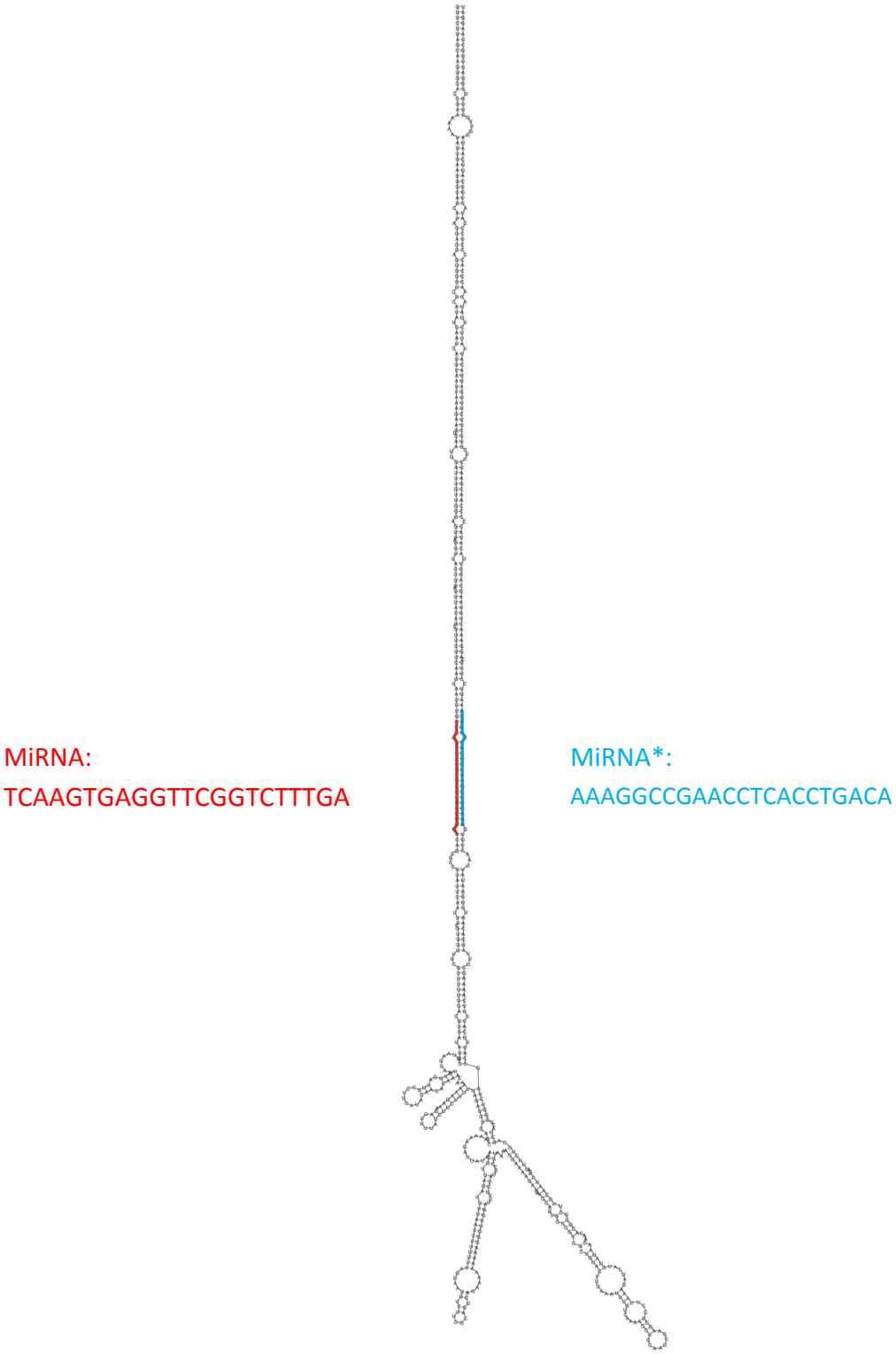

Supplemental Figure 5. Stem-loop structure of miRC1 in citrus.

Stem-loop structure was produced by RNAfold. MiRNA and miRNA* are highlighted with red and light-blue lines, respectively, with their corresponding sequences denoted beside.

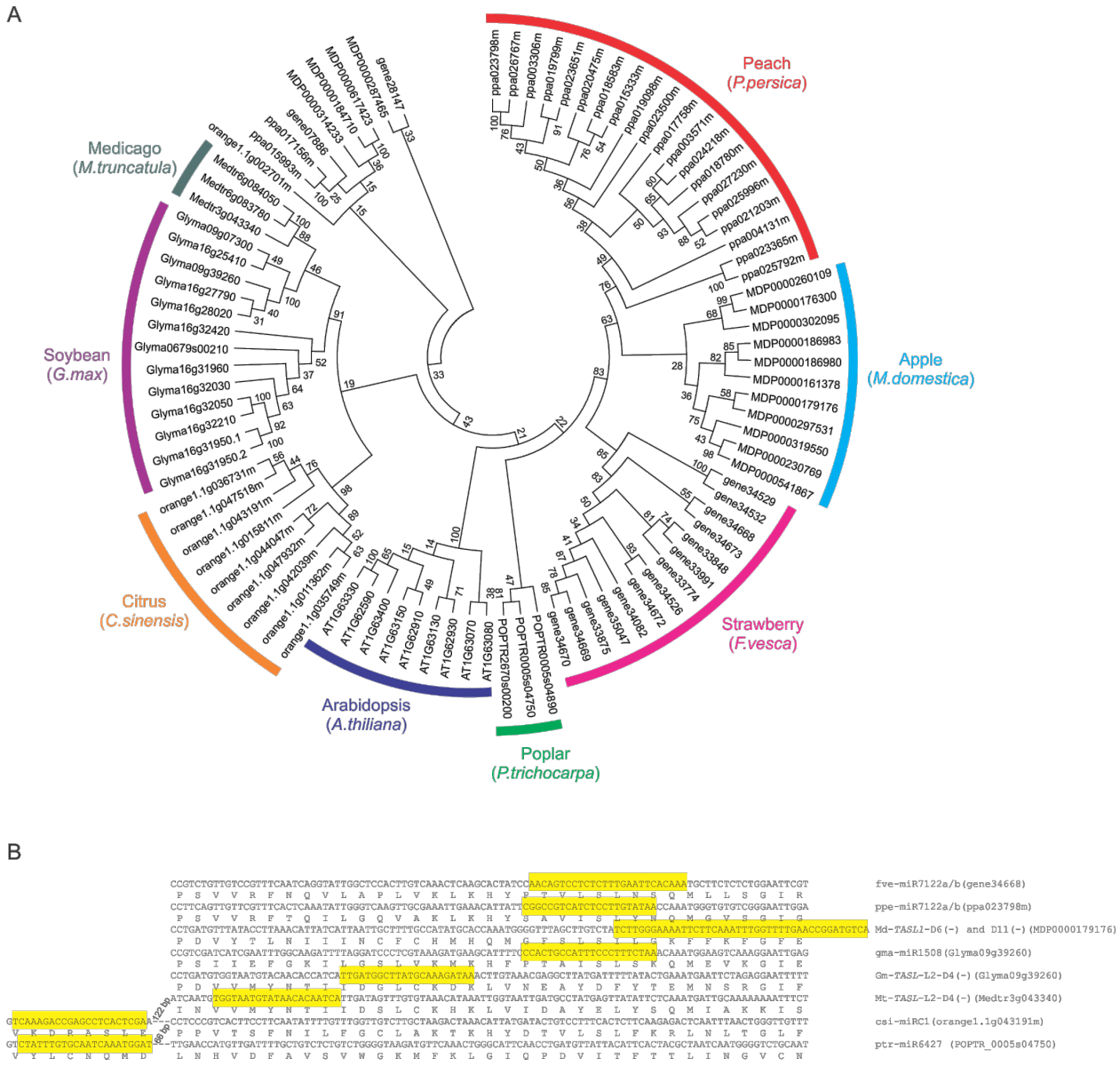

Supplemental Figure 6. Phylogenetic analysis of *PHAS PPR* genes and distribution of target sites of miRNAs or tasiRNAs along *PPR* domains.

(A) Phylogenetic analysis of *PHAS PPR* genes identified in various plants. Multiple alignment of *PPR* genes was performed with Clustalw2 with default settings with alignment results shown in Supplemental Data set 3 online. Phylogenetic tree analysis for *PPR* genes was conducted using the neighbor-joining method by MEGA5. The bootstrap consensus tree inferred from 1000 replicates is taken to represent the evolutionary history of the taxa analyzed. Branches corresponding to partitions reproduced in less than 50% bootstrap replicates are collapsed. The evolutionary distances were computed using the Poisson correction method and are in the units of the number of amino acid substitutions per site. The analysis involved 91 amino acid sequences. All positions with less than 50% site coverage were eliminated. There were a total of 560 positions in the final dataset.

(B) Distribution of target sites of miRNAs or tasiRNAs along *PPR* repeats. Target sites of miRNAs or tasiRNAs are marked in yellow.

Picea abies

Pab-miR391 (23 bp)

Initial ΔG = -58.10

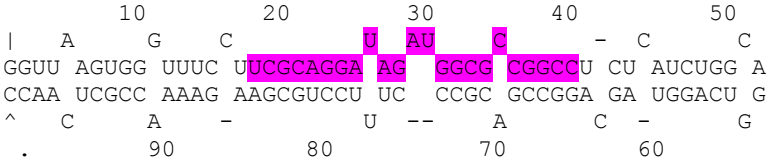

Amborella trichophoda

Atr-miR4376a (22 bp)

Initial ΔG = -57.40

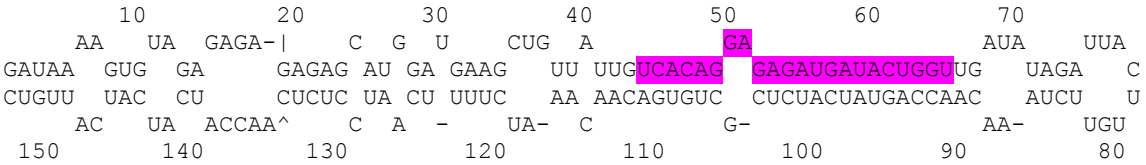

Atr-miR4376b (21 bp)

Initial ΔG = -55.90

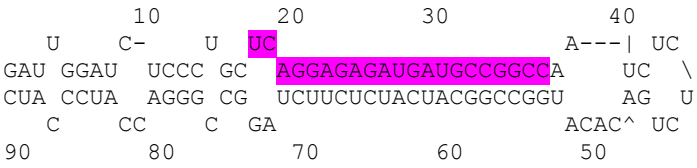

Panicum virgatum

Pvi-miR1432 (22 bp)

Initial ΔG = -63.50

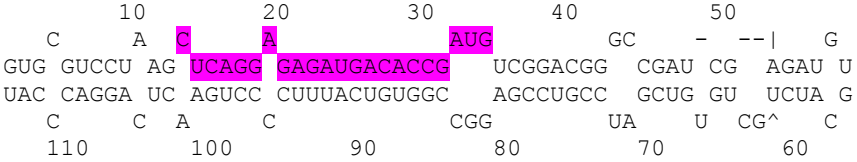

Hordeum vulgare

hvu-miR1432 (21 bp)

Initial ΔG = -66.00

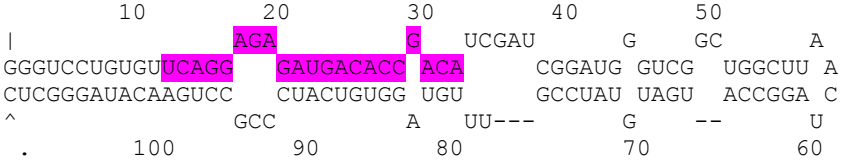

Mimulus guttatus

Mgu-miR5225 (22 bp)

Initial ΔG = -54.90

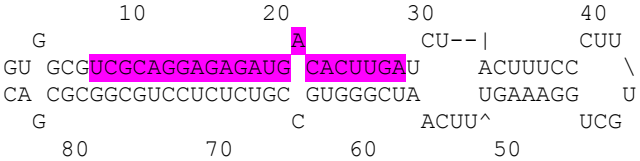

Nicotiana tabacum

Nta-miR3627 (22 bp)

Initial ΔG = -58.10

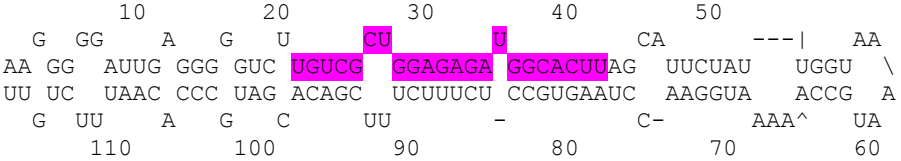

Solanum lycopersicum

Sly-miR3627

Initial ΔG = -46.70

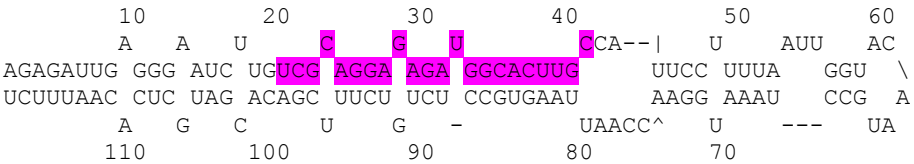

Vitis vinifera

Vvi-miR4376 (22 bp)

Initial ΔG = -54.10

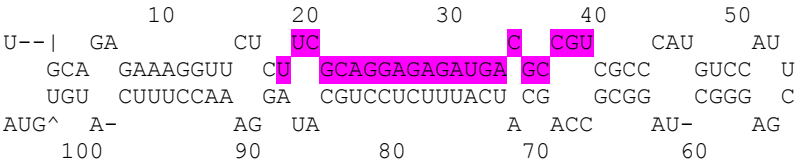

Vvi-miR5225 (22 bp)

Initial ΔG = -57.00

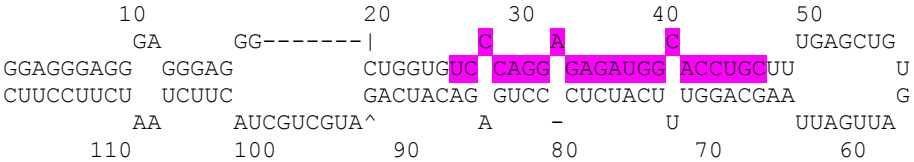

Populus trichocarpa

Ptr-miR3627 (22 bp)

Initial ΔG = -78.70

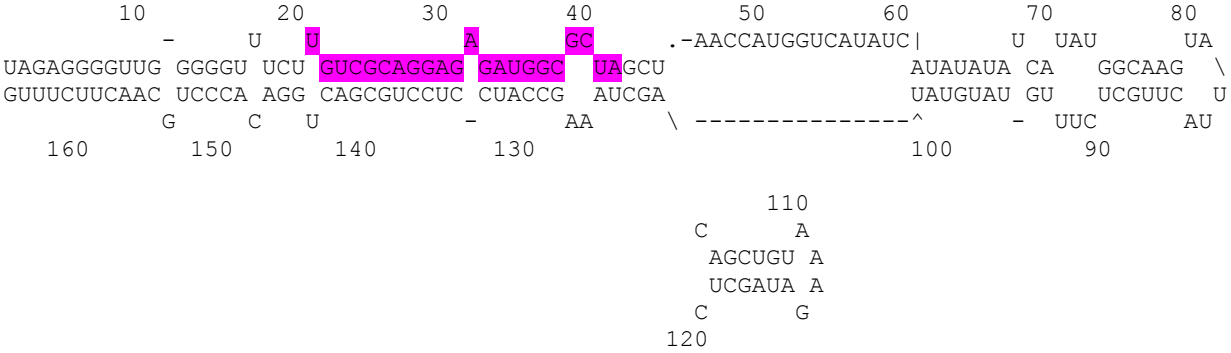

Carica papaya

Cpa-miR4376 (22 bp)

Initial ΔG = -64.30

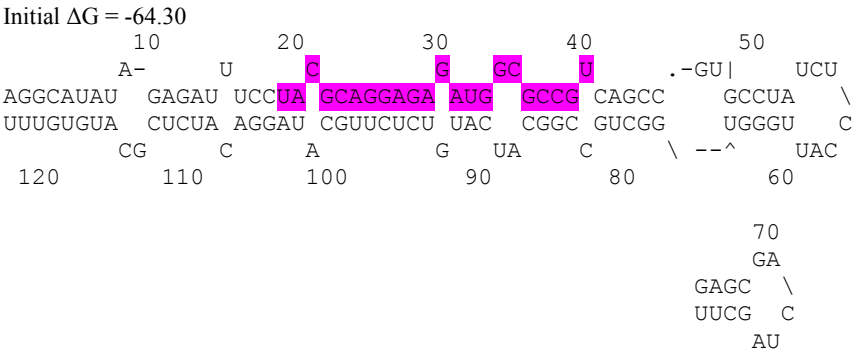

Prunus persica

Ppe-miR4376 (22 bp)

Initial ΔG = -59.10

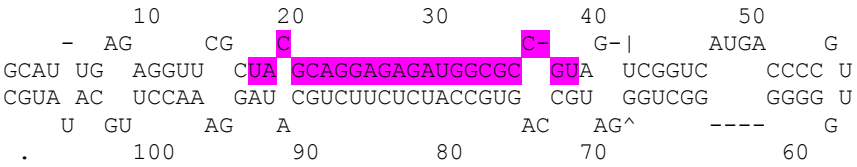

Ppe-miR3627a (21 bp)

Initial ΔG = -65.00

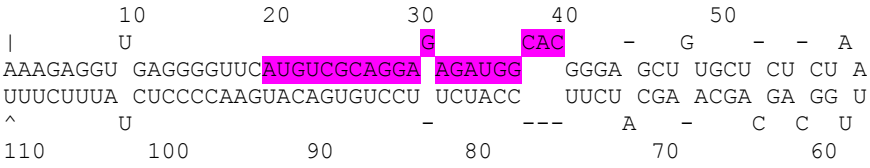

Ppe-miR3627b (*Prunus persica*, 22 bp)

Initial ΔG = -58.10

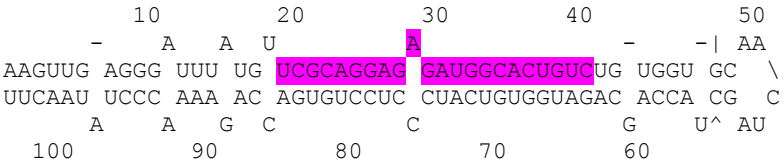

Fragaria vesca

Fve-miR3627a (22bp)

Initial ΔG = -68.50

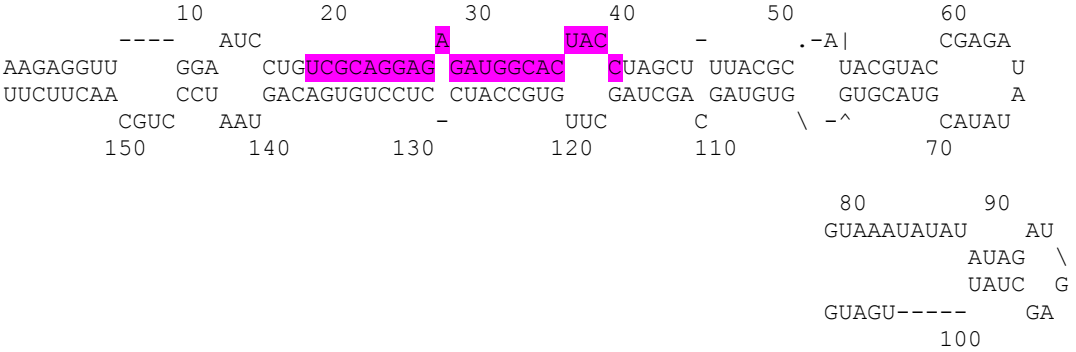

Fve-miR3627b (22bp)

Initial ΔG = -70.20

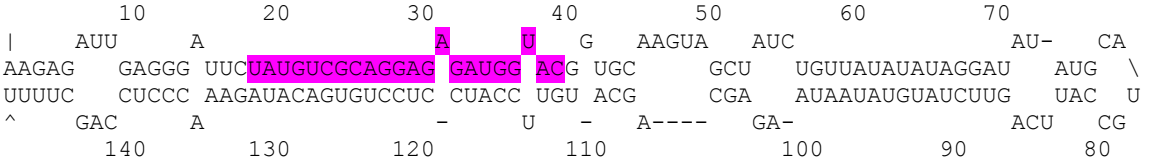

Fve-miR3627c (22bp)

Initial ΔG = -80.40

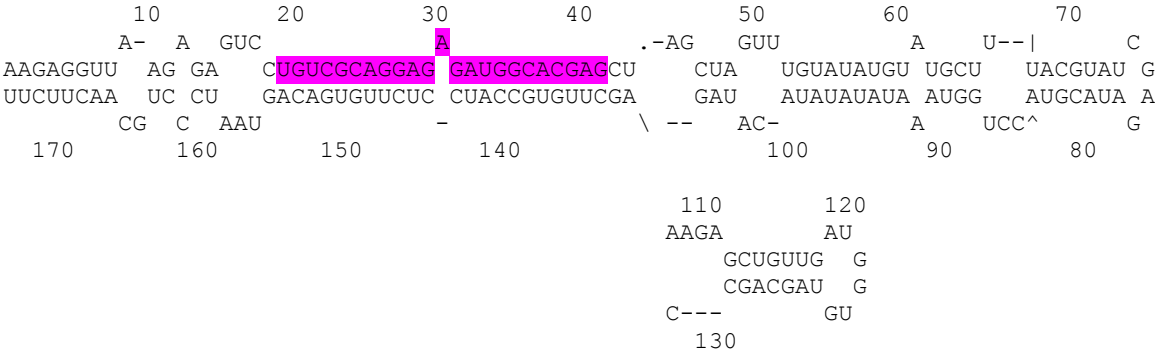

Fve-miR5225 (22bp)

Initial ΔG = -68.50

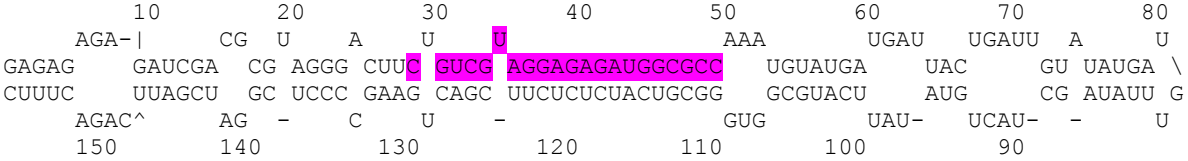

Medicago truncatula

Mtr-miR391 (21 bp)

Initial ΔG = -52.20

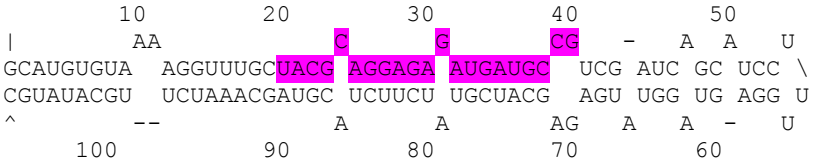

Citrus sinensis

Csi-miR3627 (22 bp)

Initial ΔG = -58.40

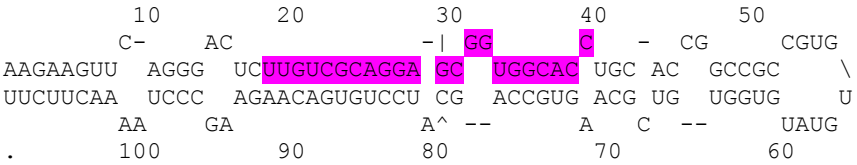

Csi-miR5225 (22 bp)

Initial ΔG = -41.30

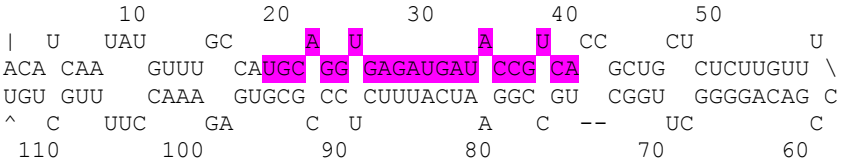

Brassica napa

Bna-miR391 (21 bp)

Initial ΔG = -40.00

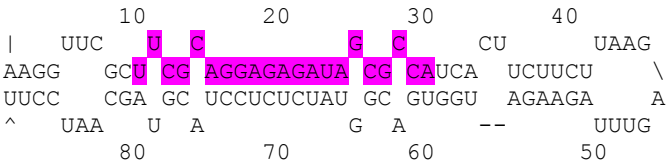

Supplemental Figure 7. Stem-loop structures of newly identified miRNA homologues of the miR4376 superfamily.

Structures were predicted using Mfold. MiRNA names were assigned according to the most similar miRNA hit retrieved by BLAST searches of the new miRNA sequence against miRbase (version 19). Mature miRNAs are highlighted in pink.

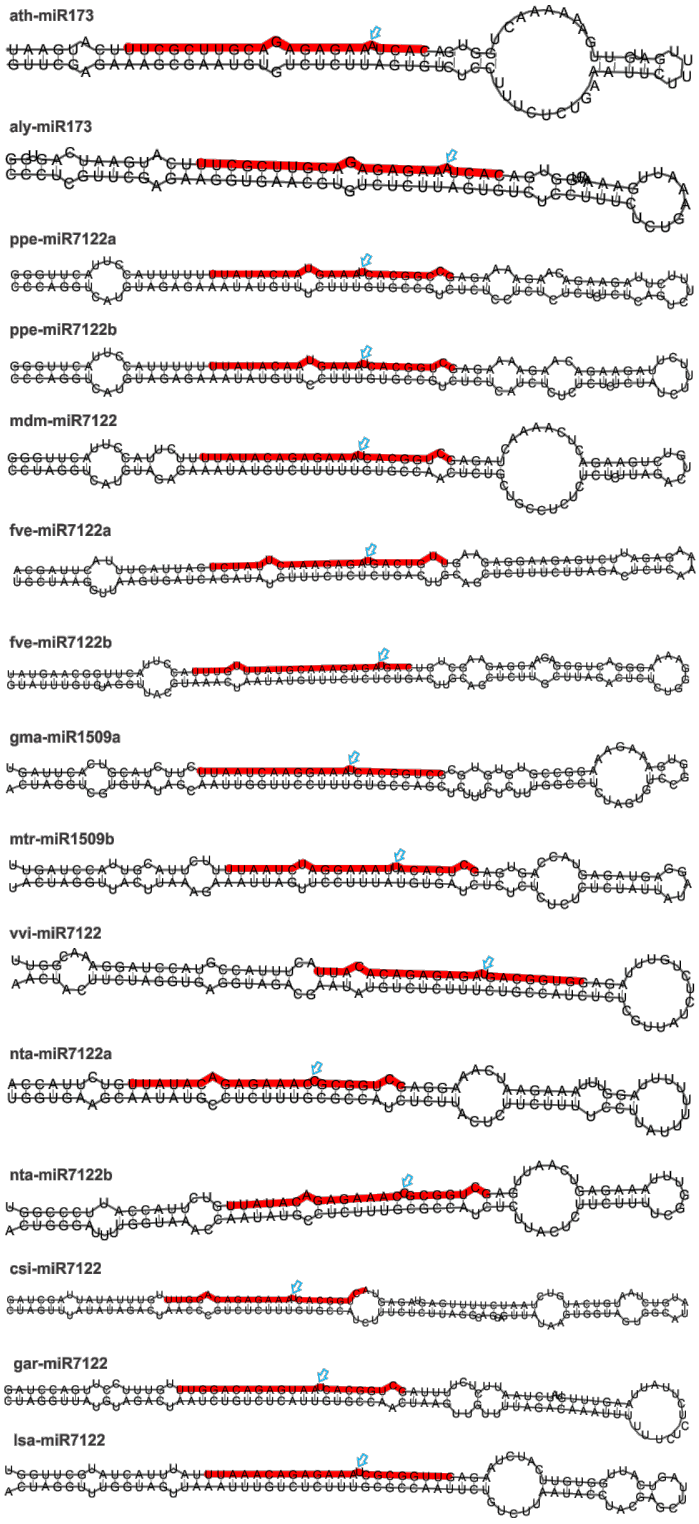

Supplemental Figure 8. Stem-loop structures of identified *MIR7122* homologues.

Stem-loop structures were produced by RNAfold. Mature miRNAs are marked with red lines; positions of bulges in miRNA/miRNA* duplex are indicated with light-blue arrows.